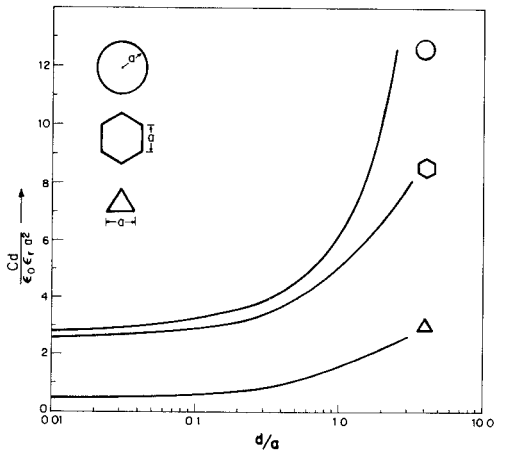

Fig. 4. Comparison of static capacitances of the hexagonal, the equilateral triangle, and the circular disk for $\epsilon_r = 10.2$

Since extensive data on the circular disk resonator are available in the literature, the resonant frequency of the commensurate hexagonal resonator can easily be computed from these data using (18). The error committed will be smaller than ± 2 percent.

V. Conclusion

This paper presents the analysis of hexagonal microstrip resonators under quasi-static approximations using the spectral domain technique. Theoretical results for their capacitance and resonant frequency are given for various dielectric constants. These values are compared with corresponding parameters of circular and triangular microstrip resonators. A simple empirical formula relates the resonant frequencies of hexagonal and circular resonators of identical dimensions. Experimental data on the hexagonal resonator agree within ± 2 percent with the computed results. Thus, the quasi-static formulation of the spectral domain technique can be utilized to predict fairly accurate resonant frequencies for the normalized hexagon side a/d less than 5.0.

References

[1] S Mao, S. Jones, and G D. Vendelin, "Millimeter-wave integrated circuits," *IEEE Trans. Microwave Theory Tech.*, vol MTT-16, pp 455–461, July 1968.

[2] T. H. Oxley, "Microwave integrated circuit techniques," *Gen. Elec Co. Ltd Engl. J. Sci. Technol.*, vol. 43, pp. 21–31, Jan. 1976

[3] G. D'Inzeo, F. Giannini, C M. Sodi, and R. Sorrentino, "Method of analysis and filtering properties of microwave planar networks," *IEEE Trans. Microwave Theory Tech* , vol. MTT-26, pp. 462–471, July 1978

[4] J. Helszajn and D. S. James, "Planar triangular resonators with magnetic walls," *IEEE Trans. Microwave Theory Tech.*, vol. MTT-26, pp. 95–100, Feb. 1978

[5] J Helszajn, D S James, and W. T Nisbet, "Circulators using planar triangular resonators," *IEEE Trans. Microwave Theory Tech.*, vol MTT-26, pp 188–193, Feb. 1979.

[6] M Cuhaci and D. S. James, "Radiation from triangular and circular resonators in microstrip," presented at 1977 *IEEE MTT-S International Microwave Symp.*, (San Diego, CA), June 1977

[7] R T. Irish, "Elliptic resonator and its use in microcircuit systems," *Electron. Lett.*, vol 7, pp 149–150, Apr. 1971.

[8] J. G. Kretzschmar, "Theoretical results for the elliptic microstrip resonators," *IEEE Trans Microwave Theory Tech* , vol. MTT-20, pp 342–343, May 1972

[9] A. K. Sharma and B Bhat, "Spectral domain analysis of elliptic microstrip disk resonators," *IEEE Trans Microwave Theory Tech* , vol MTT-28, pp. 573–576, June 1980.

[10] A. K. Sharma, "Spectral domain analysis of microstrip resonant structures," Ph.D dissertation, Indian Institute of Technology, Delhi, Dec. 1979.

[11] W. T. Nisbet and J Helszajn, "Mode chart for microstrip resonators on dielectric and magnetic substrates using a transverse resonance method," *Microwaves, Opt. Acoust.*, vol. 3, pp. 69–77, March 1979

[12] Y. Rahmat-Samii, T. Itoh, and R. Mittra, "A spectral domain analysis for solving microstrip discontinuity problems," *IEEE Trans. Microwave Theory Tech.*, vol. MTT-22, pp. 372–378, Apr. 1974.

[13] T. Itoh and R. Mittra, "A new method for calculating the capacitance of circular disk for microwave integrated circuits," *IEEE Trans. Microwave Theory Tech.*, vol. MTT-21, pp 431–432, June 1973.

[14] T. Itoh and R. Mittra, "Analysis of microstrip disk resonators," *Arch. Elek. Ubertragung* , vol. 27, pp 456–458, Nov. 1973.

[15] A. K Sharma and B Bhat, "Influence of shielding on the capacitance of shielded microstrip disk and ring structures," *Arch. Elek. Übertragung.*, vol 34, pp. 41–44, Jan. 1980.

[16] J -P Hsu, O. Kondo, T. Anada, and H. Makino, "Measurement and calculation of eigenvalues of various triplate-type microwave planar circuits," *Rec Prof. Groups, IECEJ*, paper MW 73-117, Feb 23, 1974.

S-Parameter Equivalents of Current and Voltage Noise Sources in Microwave Devices

A. D. SUTHERLAND, SENIOR MEMBER, IEEE, AND
M. W TRIPPE

***Abstract*—The representation of noise sources in terms of signal flow graph equivalents is derived, enabling one to model noisy electron devices in terms of their *S*-parameters.[1]**

I. Introduction

The characterization of the noise of electron devices at low and moderate frequencies invariably involves the introduction of series noise voltage sources or shunt noise current sources embedded in a network of impedances or admittances which includes additional controlled current or voltage sources to model the nonreciprocal behavior of the device. For example, the equivalent circuit devised by van der Ziel [1] for field-effect transistors in a common source configuration (Fig. 1) contains two noise current sources shunting the input (gate-source) and output (drain-source) terminals of that device (i.e., i_g and i_d).

Microwave devices are most conveniently characterized in terms of their scattering matrix elements (*S*-parameters). Not only are those parameters readily measured but, also, through the use of signal flow graphs, they provide a very convenient means for analysis when such devices are embedded between input and output networks which serve the purposes of providing dc bias voltages or currents, and acting as impedance transformers. It is the purpose of this short paper to demonstrate how one can also represent the presence of the noise current or voltage sources of the device in such signal flow graphs. This can be used for the purpose of analyzing the noise performance of the device in its embedding environment or, conversely, for the purpose of deducing from noise measurements the values of those equivalent *S*-parameter noise sources.

We adopt the convention prevalent in noise literature of using lower case symbols (e, i, v, etc.) to represent rms noise phasors. Because they are randomly time-dependent, they are char-

Manuscript received October 12, 1981; revised December 15, 1981. This work was supported by the National Science Foundation under Grant ENG78-00797

The authors are with the Department of Electrical Engineering, University of Florida, Gainsville, FL 32611

[1]The research leading to the results described herein was suggested by A van der Ziel.

0018-9480/82/0500-0828$00.75 ©1982 IEEE

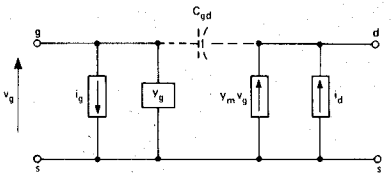

Fig. 1. Equivalent circuit due to van der Ziel for modeling the noise of a field-effect transistor. Phasor current sources i_g and i_d, in shunt with the $g-s$ and $d-s$ terminals of the device, are noise currents.

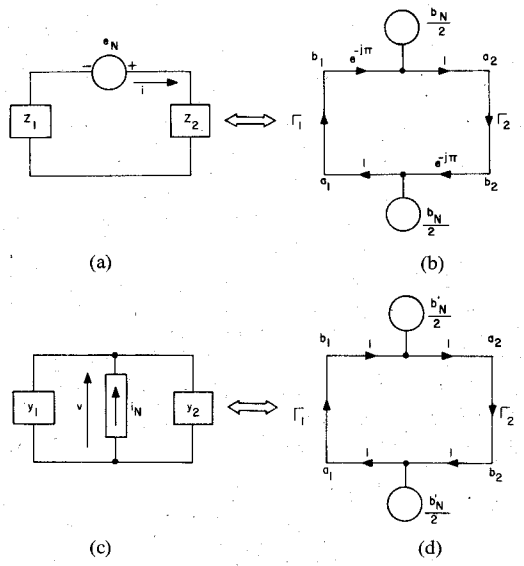

Fig. 2. (a) Phasor noise voltage source e_N seeing the impedances Z_1 and Z_2 to its left and right. (b) Signal flow graph noise model which is (a)'s equivalent. (c) Phasor noise current source i_N seeing the admittances Y_1 and Y_2 to its left and right. (d) Signal flow graph noise model which is (c)'s equivalent.

acterized experimentally in terms of time averages of their products, e.g., $\langle ii^* \rangle$, $\langle ee^* \rangle$, $\langle ei^* \rangle$, etc., the latter being a cross-correlation term.

II. Series Noise Voltage Source

Fig. 2(a) shows a phasor noise voltage e_N which sees impedances Z_1 and Z_2 connected in series with it at its left and right terminals. Fig. 2(b) shows its S-parameter equivalent, which we shall now derive by focusing attention upon the power absorbed by those impedances.

Consider the impedance Z_1. The power absorbed by it is $ii^* \operatorname{Re}\{Z_1\}$ which, in terms of e_N, becomes

$$P_1 = \left[\frac{e_N e_N^* (Z_1 + Z_1^*)}{2(Z_1 + Z_2)(Z_1^* + Z_2^*)} \right]. \tag{1}$$

To express this in S-parameter notation, introduce the reflection coefficients Γ_1 and Γ_2

$$\Gamma_1 = \left[\frac{Z_1 - Z_0}{Z_1 + Z_0} \right], \qquad \Gamma_2 = \left[\frac{Z_2 - Z_0}{Z_2 + Z_0} \right] \tag{2}$$

together with the equivalent S-parameter source b_N

$$b_N = e_N / \sqrt{Z_0} \tag{3}$$

where Z_0 is the characteristic impedance of the transmission line to which the scattering elements are referred (usually 50 Ω). Solving (2) for Z_1 and Z_2, and (3) for e_N

$$Z_1 = Z_0 \left[\frac{1+\Gamma_1}{1-\Gamma_1} \right], \qquad Z_2 = Z_0 \left[\frac{1+\Gamma_2}{1-\Gamma_2} \right], \qquad e_N = \sqrt{Z_0}\, b_N. \tag{4}$$

Substituting these results into (1), one obtains after some algebra

$$P_1 = \left[\frac{b_N}{2} \left(\frac{1-\Gamma_2}{1-\Gamma_1\Gamma_2} \right) \right] \cdot \left[\frac{b_N^*}{2} \left(\frac{1-\Gamma_2^*}{1-\Gamma_1^*\Gamma_2^*} \right) \right] \cdot (1-\Gamma_1\Gamma_1^*)$$
$$= a_1 a_1^* (1-\Gamma_1\Gamma_1^*) = a_1 a_1^* - b_1 b_1^*. \tag{5}$$

Equation (5) is precisely the result obtained from the signal flow graph of Fig. 2(b) which contains one first-order loop, namely, $\Gamma_1\Gamma_2$, and no nontouching loops for the two paths by means of which signals reach node a_1 from the *two* fully correlated noise sources present in that figure. The time-averaged noise power absorbed by Z_1 is $\langle P_1 \rangle = \langle a_1 a_1^* \rangle (1-\Gamma_1\Gamma_1^*)$.

Consideration of the power absorbed by Z_2 leads to an equation identical to (5), with all numerical subscripts interchanged. Again, the signal flow graph of Fig. 2(b) leads to the correct result for $\langle P_2 \rangle$.

III. Shunt Noise Current Source

Fig. 2(c) shows a phasor noise current i_N which sees admittances Y_1 and Y_2 connected in shunt with it to its left and right. Fig. 2(d) shows its S-parameter equivalent. Again we demonstrate this by focusing upon the power absorbed by those admittances. There are sufficient subtle differences in the outcome that it is worth repeating the derivation.

Consider the admittance Y_1. The power absorbed by it is $vv^* \operatorname{Re}\{Y_1\}$ which, expressed in terms of i_N, becomes

$$P_1 = \left[\frac{i_N i_N^* (Y_1 + Y_1^*)}{2(Y_1 + Y_2) \cdot (Y_1^* + Y_2^*)} \right]. \tag{6}$$

Introducing the reflection coefficients Γ_1 and Γ_2

$$\Gamma_1 = \left[\frac{Y_0 - Y_1}{Y_0 + Y_1} \right], \qquad \Gamma_2 = \left[\frac{Y_0 - Y_2}{Y_0 + Y_2} \right] \tag{7}$$

together with the equivalent S-parameter source b'_N

$$b'_N = i_N / \sqrt{Y_0} \tag{8}$$

one obtains as the analogs of (4)

$$Y_1 = Y_0 \left[\frac{1-\Gamma_1}{1+\Gamma_1} \right], \qquad Y_2 = Y_0 \left[\frac{1-\Gamma_2}{1+\Gamma_2} \right], \qquad i_N = \sqrt{Y_0}\, b'_N. \tag{9}$$

Again substituting these into (6), and performing similar algebra,

$$P_1 = \left[\frac{b'_N}{2} \left(\frac{1+\Gamma_2}{1-\Gamma_1\Gamma_2} \right) \right] \cdot \left[\frac{b'^*_N}{2} \left(\frac{1+\Gamma_2^*}{1-\Gamma_1^*\Gamma_2^*} \right) \right] \cdot (1-\Gamma_1\Gamma_1^*)$$
$$= a_1 a_1^* (1-\Gamma_1\Gamma_1^*) = a_1 a_1^* - b_1 b_1^*. \tag{10}$$

Equation (10) is precisely the result obtained from the signal flow graph of Fig. 2(d). Again, the time-averaged noise power absorbed by Y_1 is $\langle P_1 \rangle = \langle a_1 a_1^* \rangle (1-\Gamma_1\Gamma_1^*)$, and a similar result is obtained for $\langle P_2 \rangle$ simply by interchanging the subscripts in (10).

In addition to the different manner in which the S-parameter equivalent noise sources b_N and b'_N are defined, compare (3) and (8), note the subtle difference in the two results. The *signs* in the numerator of the bracketed expressions defining a_1 in (5) and (10) differ. This is due to the reversal of the signs relating Z_1 and Z_2 to Γ_1 and Γ_2 in (4) and the corresponding expressions relating Y_1 and Y_2 to those same reflection coefficients in (9). Thus, whereas Fig. 2(b) includes two phase factors $\exp(-j\pi)$, those phase factors are missing in Fig. 2(d).

IV. Conclusions

We have shown that it is possible to replace the series voltage or shunt current noise sources which appear in the lumped circuits for modeling the noise of solid state devices at low and

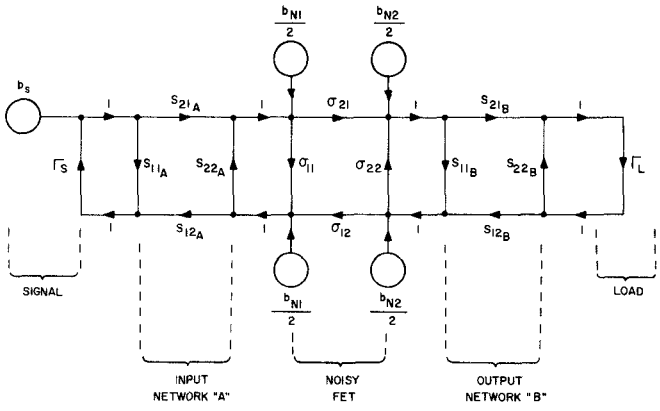

Fig. 3. Signal flow graph equivalent to the noisy FET of Fig. 1, embedded between input and output networks which provide dc bias as well as impedance transformation The noise sources b_{N1} and b_{N2} are the S-parameter equivalents of the noise current sources i_g and i_d of the FET model of Fig. 1. The σ's represent the four S-parameters of the FET.

moderate frequencies with signal flow graph equivalents, so that the noise performance of the device can be analyzed in terms of its S-parameters. Fig. 3, for example, shows the signal flow graph which results when a field-effect transistor, whose moderate-frequency noise model is that devised by van der Ziel (Fig. 1), is embedded between input and output linear networks serving to provide dc bias to the device as well as performing the function of transforming impedances. The source b_S in Fig. 3 represents a *signal* source, not a noise source, and is defined in the usual manner [2]. That is to say

$$b_S = \frac{V_S\sqrt{Z_0}}{Z_S + Z_0}, \qquad \Gamma_s = \frac{Z_S - Z_0}{Z_S + Z_0}. \tag{11}$$

Since, at microwave frequencies, the "natural" measurable parameters of a solid-state device, as well as those of the linear networks in which it is embedded, are the S-parameters, it seems to the authors that the "natural" manner in which to characterize the noise sources of the device is that which has been developed in this short paper. In a sequel paper, we shall describe the results of experiments with a GaAs MESFET at 3 GHz still in progress which have as their goal the direct measurement of the noises $\langle b_{N1}b_{N1}^*\rangle$, $\langle b_{N2}b_{N2}^*\rangle$, and their cross-correlation $\langle b_{N1}b_{N2}^*\rangle$ (both real and imaginary parts) of the sources shown in Fig. 3.

V. Addendum

While the above paper was under second review following revision, Hecken [3] published an important paper also dealing with the use of S-parameters to characterize the noise of active devices. A brief comment on how his approach differs from the above is in order. Whereas our equivalent noise sources relate directly to the current and/or voltage sources encountered in moderate frequency models for device noise, Hecken simply includes sources contributing to the "b"-waves emanating from each port of the device. There is nothing wrong with that approach. However, it cannot be used to interpret the physical mechanisms accounting for the noise. Inspection of Fig. 3, for example, reveals that both b_{N1} and b_{N2} (consequently van der Ziel's current sources i_g and i_d in Fig. 1) contribute to the noise emanating from both ports of the noisy FET, even if those ports see perfect impendance matches connected to them. In other words, Hecken's B_{q1} and B_{q2} are due to an admixture of the contributions from two differing physical mechanisms for the noise, and measurement of them in the neat way that he describes will provide no physical insight as to their cause because, with both ports matched, only his noise source B_{q2} contributes to the noise emanating from port 2 and vice-versa.

References

[1] A. van der Ziel, *Noise: Sources, Characterization, Measurement*. Englewood Cliffs, NJ: Prentice-Hall, 1970, ch. 7, p. 124.
[2] *S-Parameter Design*. Hewlett-Packard Application Note 154, p 124, Apr 1972.
[3] R. P. Hecken, "Analysis of linear noisy two-ports using scattering waves," *IEEE Trans. Microwave Theory Tech.*, vol. MTT-29, pp. 997–1004, Oct. 1981

On the Inherent Noise of an Ideal Two-Port Isolator

A. D. SUTHERLAND, SENIOR MEMBER, IEEE

Abstract—**The inherent noise of an ideal isolator, predicted by Siegman from a simple thermodynamic argument, is verified by examining in detail the behavior of a common two-port isolator configuration, insofar as its sources of noise are concerned. Siegman's conclusion that any ideal isolator is the equivalent of a terminated three-port circulator is vindicated.**

I. Introduction

In 1961 Siegman [1] concluded from a thermodynamic argument that all isolators are the equivalent of terminated circulators insofar as their inherent noise is concerned. That argument is so neat that it is worth reviewing, especially since it appeared in a 20-year-old journal not likely to be available to the reader. Fig. 1(a) shows an ideal isolator which transmits a signal from port 1 to port 2 without attenuation, but attenuates perfectly any signal incident upon port 2 without reflection. Siegman described the following paradox. Suppose port 1 is matched with a termination at a *cold* temperature T_1 while port 2 is similarly matched at a *hot* temperature T_2. Then *all* of the Nyquist noise power $kT_1\Delta f$ from the cold resistor at port 1 reaches and is absorbed by the matched load at port 2, but *none* of the Nyquist noise power $kT_2\Delta f$ from the hot resistor at port 2 reaches its counterpart at port 1. This is clearly a violation of the second law of thermodynamics since we have a continuous transfer of heat from a cold source to a hot sink. Based on this paradox, Siegman argued that an ideal isolator must be modeled as an ideal three-port circulator with its port 3 resistively matched, as shown in Fig. 1(b), that termination accounting for the dissipative losses *inherent* in an isolator in order to produce its nonreciprocal action. This clearly removes the paradox because now the additional Nyquist noise power $kT_3\Delta f$ exits port 1 and is absorbed by the cold termination there. A signal flow analysis of the latter situation reveals that the *net* noise power entering all three ports sums to zero, and the second law is satisfied.

One concludes from the above argument that the inherent thermal noise of any isolator is Nyquist noise $kT\Delta f$ exiting from port 1 only. That this is indeed the case is not intuitively obvious

Manuscript received September 28, 1981; revised December 15, 1981. This work was supported by the National Science Foundation under Grant ECS-8007623.

The author is with the Department of Electrical Engineering, University of Florida, Gainseville, FL 32611

0018-9480/82/0500-0830$00.75 ©1982 IEEE